needed. We have developed two helper components that provide this ability. The first kind is similar to eye patching.[5] It hides half of the screen or limits the view to a window centered or shifted around the eye-gaze location or the interaction tool. We can displace the virtual objects in the non-neglected space by shifting this window to the left in different spatial frames of reference: the patient's hand or eye-gaze. Last, it was shown that optokinetic stimulation could increase awareness toward the neglected space.[5] Our system can dynamically superimpose a flow of dots moving toward the neglected space or from the eye-gaze location to a specific virtual object.

*Haptic helper components.* Considering that patients with a heavy impairment have difficulties to finely control their arms, it was necessary to find a solution to facilitate grabbing. We are using haptic magnets in the virtual object that should be reached. The patient's hand is guided when relatively close to the target. Another haptic helper consists of inverting the lateral axis of the interaction device. It was shown that changing the somatic representation of a patient's own body has a positive impact[6] on the neglect because of the associated arousal effect. We want to study the impact of discrepancies between visual and somatic representations.

*Pencils and paper test*

*Recorded data.* Our system can record the interactions, eye-gaze, virtual world events and the state of the virtual objects with a timestamp for replay purpose. The recorded interactions are the position, forces and state of the Phantom. The events and the recorded data are different for each task. In the case of the virtual sushi bar, it consists of the position of each sushi, the rotation speed and direction of the turntable and the target sushi.

*Common points.* The pencil and paper tests have several common points. Notably the setup is the same for all tasks: a paper is placed on a table and the Phantom device is used to control the pencil. A dynamic friction is applied when the pencil is on the paper to ease the drawing. The patient needs to touch the virtual table to validate his choice and to move on to the next task. Trials are shuffled but the order is recorded for the analysis of the results.

*Line bisection.* The line bisection task consists of marking the middle of a line (Fig. 4). There are very long (25 cm), long (20 cm), medium (13 cm) and short (5 cm) lines. They can be centered or place to the either side of the sheet. For each trial, these characteristics, the position of the mark and the validation time are recorded.

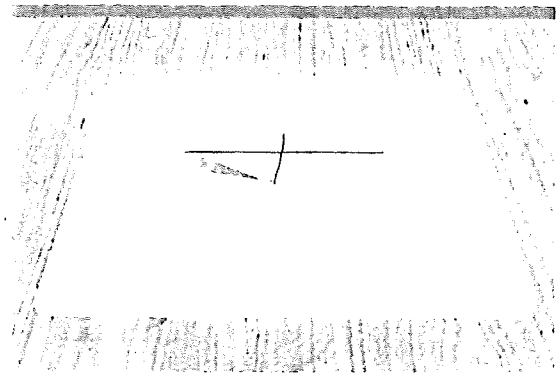

FIG. 4. Virtual line bisection.

*Drawing copy.* The drawing copy task consists in copying a reference drawing (Fig. 5). Several familiar objects have to be copied. Contrary to the actual pencil and paper test, we made it impossible to write on the same side of the reference model. The strokes drawn by the patient are recorded with timestamps.

*Target cancellation.* The target cancellation task consists of marking short lines scattered on the test sheet. The patients with neglect start in the right side and don't seem to have a predetermined scanning pattern. On the other hand, healthy subjects use a left to right, top to bottom pattern to mark the targets. The pattern is more significant than the number of missed targets[2] and can be determined with the eye-gaze tracking system. The recorded data are the position of the marks, the position and state (checked, unchecked) of each target.

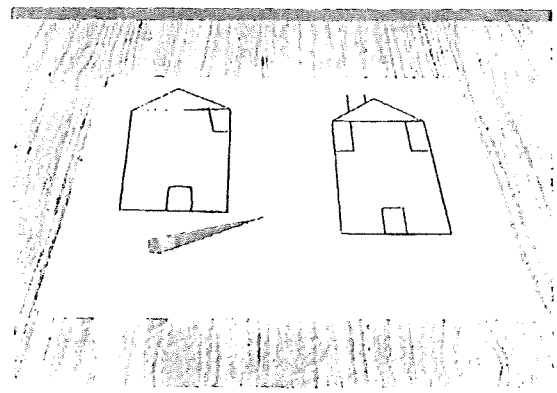

FIG. 5. Virtual drawing.

## CONCLUSION

The proposed system combines a stereovision enabled virtual world with force feedback and spatial sounds to achieve a high degree of immersion. The system provides more information about the way a patient is executing a task. For instance, the eye-gaze tracking system can record the scanning pattern. This is a particularly interesting feature because it was shown that the scanning pattern is a very significant measure. Also, the system can be used to test the efficiency of techniques such as optokinetic stimulation, eye-patching and audio hints.

## REFERENCES

1. Heilman, K.M., et al. (1985). *Neglect and related disorders*. Oxford: Oxford University Press.
2. Azouvi, P., et al. (2002). Sensitivity of clinical and behavioral tests of spatial neglect after right hemisphere stroke. *J Neurol Neurosurg Psychiatry* 73: 160–166.
3. Halligan, P.W., & Marshall, J.C. (1991). Left neglect for near but not for far space in man. *Nature* 350: 498–492.
4. Shinsha, N., & Ishigami, S. (1999). Rehabilitation approach to patients with unilateral spatial neglect. *Topics in Stroke Rehabilitation* 6:1–14.
5. Butter, C.M., & Kirsch, N. (1992). Combined and separate effects of eye patching and visual stimulation on unilateral neglect following stroke. *Arch Phys Med Rehabil* 73:1133–1136.
6. Bartolomeo, P., et al. (2004). The influence of limb crossing on left tactile extinction. *J Neural Neurosurg Psychiatry* 75:49–46.

Address reprint requests to:
*Dr. Kenji Baheux*
*Graduate School of Engineering*
*Tohoku University*
*Aoba6-6-05, Aramaki, Aoba-ku*
*Sendai 980-8579, Japan*

*E-mail:* kenji.baheux@ieee.org

# Indirect Flow Rate Estimation of the NEDO PI Gyro Pump for Chronic BVAD Experiments

Daisuke Ogawa,*|| Makoto Yoshizawa,† Akira Tanaka,‡ Ken-ichi Abe,§ Paul Olegario,* Tadashi Motomura,|| Hisashi Okubo,|| Takeshi Oda,|| Toshiya Okahisa,|| Stephen R. Igo,|| and Yukihiko Nose||

**In totally implantable ventricular assist device systems, measuring flow rate of the pump is necessary to ensure proper operation of the pump in response to the recipient's condition or pump malfunction. To avoid problems associated with the use of flow probes, several methods for estimating flow rate of a rotary blood pump used as a ventricular assist device have been studied. In the present study, we have performed a chronic animal experiment with two NEDO PI gyro pumps as the biventricular assist device for 63 days to evaluate our estimation method by comparing the estimated flow rate with the measured one every 2 days. Up to 15 days after identification of the parameters, our estimations were accurate. Errors increased during postoperation days 20 to 30. Meanwhile, their correlation coefficient *r* was higher than 0.9 in all the acquired data, and estimated flow rate could simulate the profile of the measured one. *ASAIO Journal* 2006; 52:266–271.**

In cardiac patients, ventricular assist devices (VADs) have been developed and clinically applied for many years. Recently, totally implantable VAD systems have been used to improve a patient's quality of life. In such systems, the pump flow rate provides important information for proper pump operation in response to the recipient's condition or pump malfunction.

Usually, ultrasound and electromagnetic flow probes are used for monitoring; however, these sensors are sometimes too bulky for implantation and require additional power consumption. To avoid such problems, methods for estimating flow rate of the rotary blood pump used as a VAD have been studied.[1–5] These methods can be realized by processing the rotational speed of the impeller and power consumption of the actuator, which are easy to measure. An estimation method with an autoregressive exogenous (ARX) model also has been developed, and studies have demonstrated its capability to replace the flow meter in a mock circulatory system and acute animal experiments.[6,7]

To apply this method to clinical use, the evaluation in long-term use *in vivo* is necessary, because the time-varying condition of the circulatory system may affect the accuracy of the estimation. Ayre *et al.*[8] reported a successful result in long-term experiments but concluded that the result depended on the flat P-Q curve in the static characteristic of the pump. This implies that evaluation with other pumps should be done if we apply this method to other pumps. Tsukiya *et al.*[9] succeeded in estimating waveforms and mentioned that the method of suppressing noise in the motor current is desired. Neither of these studies reported the chronic change in the accuracy of the estimated flow rate. Other methods[4,5] were tested only in the mock circulation or acute experiment; thus, more tests in practical situations should be performed.

This author's research group developed a much smaller centrifugal pump to make it more implantable[10]; however, the characteristics of the small implantable pumps may be so different from those of other traditional pumps that it is necessary to ascertain whether this method of estimating flow rate is still valid for long-term implantation in animals. In the present study, a long-term animal study was performed with two implanted NEDO PI pumps (**Figure 1**) for 63 days, to compare the estimated flow rate with the measured flow rate in terms of the average value and similarity of the waveform.

## Materials and Methods

### *Estimation Using ARX Model*

The flow rate estimation method is based on the method proposed by Yoshizawa *et al.*[6] To correlate flow rate with rotational speed, supplied power, and other indexes, an ARX model was used given by:

$$y(k) + \sum_{i=1}^{L} a_i y(k-i) = \sum_{j=1}^{3} \sum_{i=0}^{M_j} b_{ij} u_j(k-i) + w(k) \qquad (1).$$

Inputs $u_j(k)$ and output $y(k)$ are written as $[u_1 u_2 u_3] = [V/N\ N\ K]$, and $Q(k)$, where $Q(k)$, $I$, $N$ are flow rate, electric current, and rotational speed, respectively. $k$ is a notation of the discrete time. $w(k)$ is the residue assumed to be white noise. $V$ is a constant voltage of 15 V. The first and second terms in inputs, $V/N$ and $N$, were derived from the static characteristic of the pump and the circulatory system.[5] With these terms, the flow rate curve can be represented in a practical range. On the other hand, in cases where the VAD drains blood from the left ventricle, pulsatile movement of the left ventricle changes the preload of the pump. The static model cannot represent this dynamic characteristic. We replaced each term in the static characteristic with time series data and obtained the ARX model, which can represent the dynamic characteristic. With this method, a waveform that reflects the dynamics can be simulated more precisely.

The third term $K$ is given by

From the *Graduate School of Engineering, Tohoku University, Sendai, Japan; †Information Synergy Center, Tohoku University, Sendai, Japan; ‡Faculty of Symbiotic Systems Science, Fukushima University, Fukushima, Japan; §College of Engineering, Nihon University, Koriyama, Japan; ||Michael E. DeBakey Department of Surgery, Baylor College of Medicine, Houston, Texas.

Submitted for consideration August 2005; accepted for publication in revised form February 2006.

Reprint requests: Dr. Yukihiko Nosé, Michael E. DeBakey Department of Surgery, Baylor College of Medicine, One Baylor Plaza, Houston, TX 77030.

DOI: 10.1097/01.mat.0000219066.21197.34

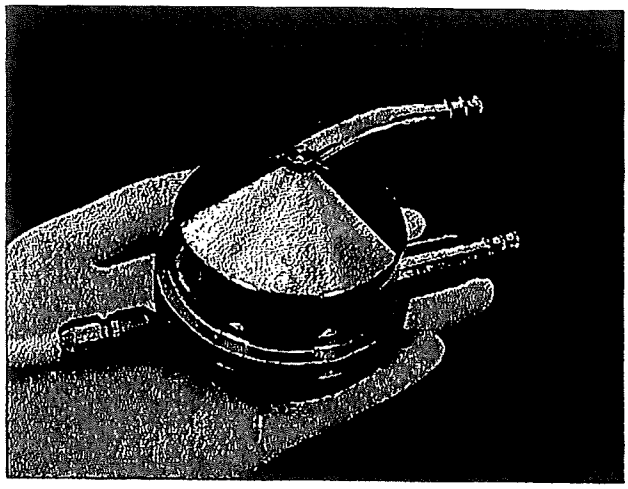

Figure 1. NEDO PI centrifugal pump (height of the housing: 37 mm, diameter: 55 mm).

$$K(k) = \frac{\sum_{i=1}^{n} N(k-i+1)}{\sum_{i=1}^{n} VI(k-i+1)} \quad (2)$$

and represents a steady-state gain from supplied power to rotational speed. The steady-state gain $K$ was introduced to compensate for changes in the physiological condition such as viscosity of blood; for example, when the viscosity of blood increases, then the actuator needs more power consumption to keep the same level of flow rate. Meanwhile, power consumption increases when the flow rate is larger. These two facts mean that we cannot judge the change in flow rate only with the power consumption. To detect the change in viscosity independently, our method uses the ratio between the rotational speed and power consumption. Effectiveness of this term has been proven in the previous studies.[6,7] Taking into account the sampling rate, the orders of the model $L$, $M_j$, and $n$ in this paper were 10, [8 8 1] and 3,000, respectively.

Figure 2 shows the idea of flow rate estimation. In practical use, $y(k)$ can be calculated with measured $u_j(k)$ and parameters $a_i$ and $b_{ij}$. These parameters were identified with measured $u_j(k)$ and $y(k)$ in advance, with MATLAB R14 (Mathworks Inc., Natick, MA) and the System Identification Toolbox. The data for identification of parameters should be measured in a mock circulation, animal experiments, or during surgery.

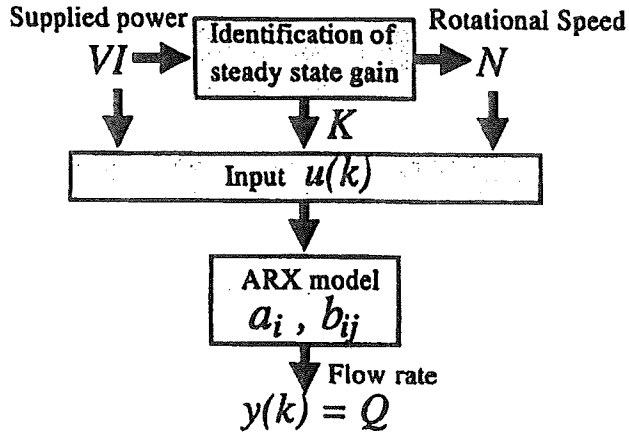


Figure 2. Idea of flow rate estimation based on supplied power and rotational speed.

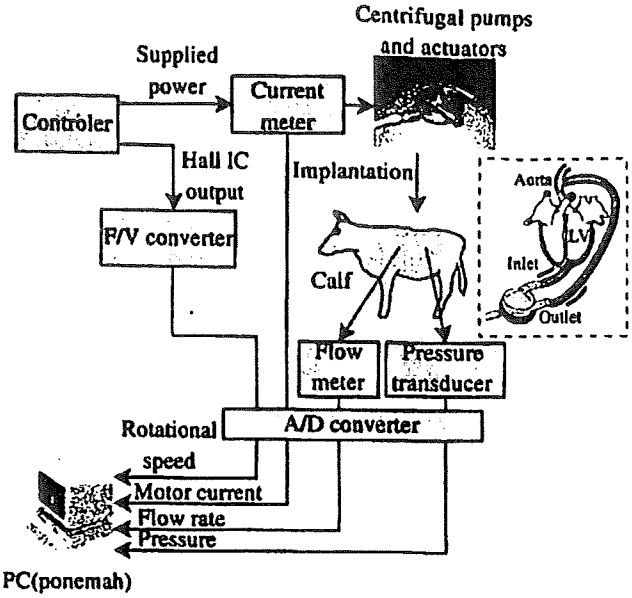


Figure 3. Experimental setup. Measurement system and connection of the LVAD and the natural heart.

### *Preprocessing*

To eliminate noise and unfavorable components in electric current waveform, the wavelet filtering method was applied. Wavelet decomposition with bi-orthogonal function was applied to the current waveform; then, the detail coefficients smaller than the threshold level were ignored, after which the current waveform was reconstructed with the same wavelet function. All calculations were performed with MATLAB R14 and the Wavelet Toolbox. The filtering was performed using the function "wden" and mother wavelet "bior4.4" in the wavelet toolbox. For details, refer to the book.[11]

At first, to improve the accuracy of the estimation, a low-pass filter (LPF) was applied to suppress a small vibration included in the electric current. However, the LPF also removed steep changes in the rising edge of the waveform and the estimation error did not decrease. For improvement, wavelet filtering was applied, which was suitable for processing nonstationary signals

### *Experiment*

Schematic illustration of the measurement system for the animal experiment is shown in Figure 3. In this system, the rotational speed was manually adjusted to keep a certain level of flow rate.

Two NEDO PI pumps were implanted in a calf as the left VAD (LVAD) and the right VAD (RVAD), respectively. The calf was healthy from the beginning of the experiment to POD 61. In the LVAD, blood was drained from the left ventricular apex with a titanium tip and a cannula connected to the inlet of the pump. The outlet of the pump was grafted to the descending

aorta, as shown in Figure 3. An ultrasonic flow probe (Transonic. Inc, Ithaca, NY) was placed on the graft.

Flow rate, electric current, and rotational speed were measured at 1 kHz and discretized to make the sampling rate 500 Hz every 2 days while the calf was in a sitting position, except for day (POD) 19.

The care and use of the animal reported in this study were approved by the Baylor College of Medicine Animal Protocol Review Committee.

### *Evaluation of Estimation Method*

The datasets obtained on POD 11 and 13 were used to identify the parameters of the ARX model $a_i$ and $b_{ij}$. The data consist of four sets of the measured data that were obtained while the rotational speed of the left pump ($N_L$) was set to 1,780 rpm, 1,700 rpm (POD 11), 1,870 rpm, and 1,700 rpm (POD 13), respectively. These operating points were in the normal range on PODs 11 and 13. The length of each data measurement was 20 seconds. The average heart rate was about 90 bpm in these four sets of data, for a total of 120 cardiac cycles, which we considered an adequate amount of data for our method.

The accuracy of the estimation was evaluated with root mean square error (*r.m.s.e*), correlation (*r*) and bias (*bias*):

$$r.m.s.e. = \sqrt{\frac{1}{K_D}\sum_{k=1}^{K_D}\{y(k) - \hat{y}(k)\}^2} \tag{3}$$

$$r = \frac{\sum_{k=1}^{K_D}\{y(k) - \bar{y}\}\{y(k) - \hat{y}\}}{\sqrt{\sum_{k=1}^{K_D}\{y(k) - \bar{y}\}^2 \sum_{k=1}^{K_D}\{\hat{y}(k) - \hat{y}\}^2}} \tag{4}$$

$$\text{bias} = \hat{y} - \bar{y} \tag{5}$$

where $\hat{y}$ is the estimate of $y$, $\bar{y}$ is the mean value of $y$, $\bar{y}$ is the mean value of $\hat{y}$, and $K_D$ is the number of data.

## Results

### *Result of Preprocessing*

Figure 4 shows the comparison between the electric current waveforms with and without preprocessing, using wavelet filtering. In the original waveform, interesting high-frequency noise components can be found. However, they were removed, and only the profile of the original waveform was obtained by the preprocessing.

### *Evaluation of Waveform Estimation*

Figure 5(a) shows waveforms of the measured electric current, rotational speed, flow rate of the left pump, and the estimated flow rate. Table 1 shows *r.m.s.e.*, *r*, and *bias* in this case. The representative results in the beginning, middle, and end stage of the experiment are shown in Figure 5(b). An unfavorable event of reverse flow occurred on POD 17, which indicated the value of flow rate was lower than 0 l/min, thus implying that the pump was not working efficiently. Table 1 also shows *r.m.s.e*, *r*, and *bias* in the cases of POD 17, 37, and 57.

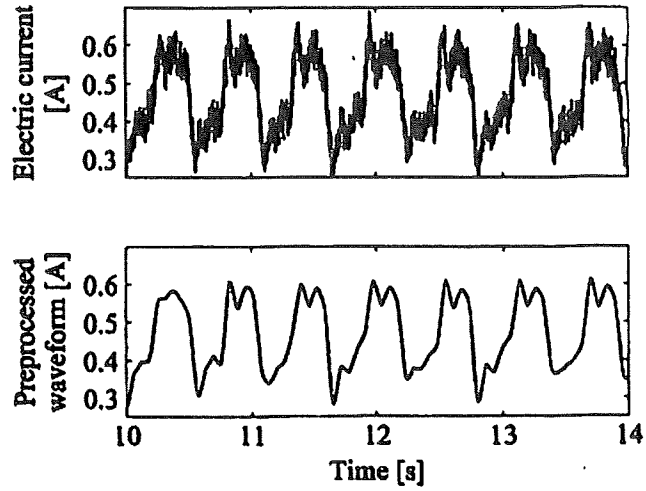


Figure 4. Original and preprocessed electric current waveforms (*top:* original waveform; *bottom:* preprocessed waveform with wavelet filtering).

### *Evaluation in Long-term Use*

Figure 6 shows the trend of *r.m.s.e.*, *r*, and *bias* during the experiment. This figure also shows the comparison between two kinds of preprocessing, which were done by the Butterworth LPF (cutoff frequency: 400 Hz) and the wavelet filter. In the case of the LPF, the orders of the model $L$, $M_j$, and $n$ were 0, [5 5 1], and 3,000, respectively. These values are determined by trial and error, avoiding the divergence of the estimated value. In the beginning of the experiment, *r.m.s.e.* and *bias* were not so large. After that, they tended to increase as the days passed. Meanwhile, $r$ was higher than 0.90 in all the datasets. Wavelet filtering made $r$ close to 1.0 and slightly improved *r.m.s.e.* and *bias*.

Rotational speed $N$ was manually changed to keep a certain level in flow rate during the experiment. The trend of the rotational speed and pump flow during the experiment is shown in Figure 7. As references, the trend of physiological data (aortic pressure; AoP, and total flow measured at the pulmonary artery) and gain $K$ are shown in Figure 8.

## Discussion

### *Evaluation of Waveform Estimation*

Figures 5(a) and (b) show that the estimated flow rate could simulate the profile of the measured one with good accuracy. As shown in Figure 7, $r$ was high enough throughout the experiment, and wavelet filtering improved the accuracy of the estimation.

Previous studies[12] mentioned that electric current was affected by change in preload. This is the origin of the oscillation in the electric current. Meanwhile, the impeller of the NEDO PI pump levitated by hydraulic force,[13] and thus, the impeller swung periodically, which might be the reason for the small vibration in the electric current waveform. Preprocessing with wavelet transform could remove only the small vibration in waveforms without phase delay and preserve smooth changes, which was necessary to simulate the measured flow rate. This was probably the reason

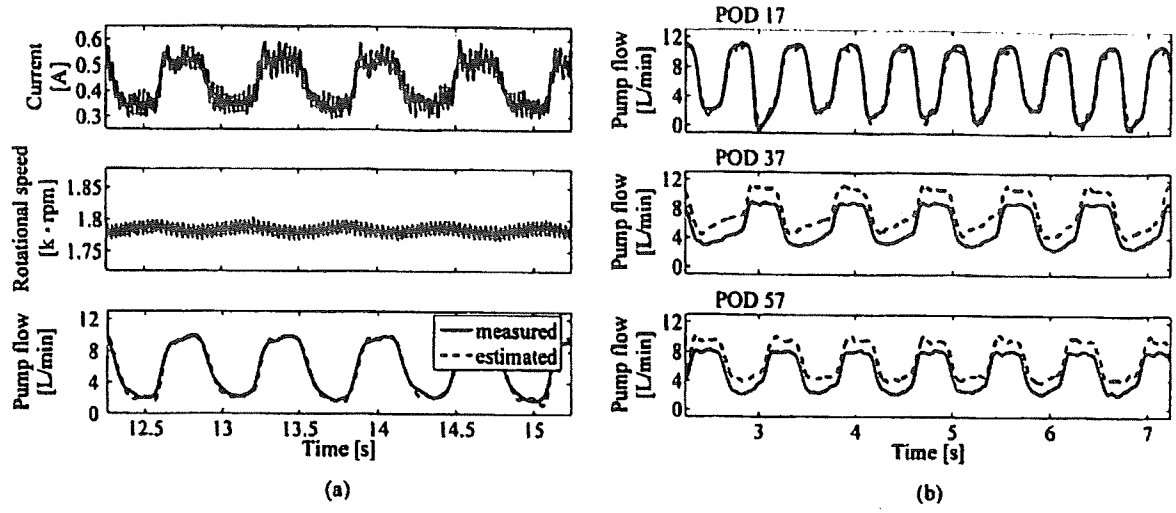


Figure 5. Comparison between the measured and the estimated flow rate (*solid line:* the measured waveform; *dotted line:* the estimated waveform). (a), Pump flow and other measured data on POD 11; (b), the measured and the estimated flow rate on POD 17, 37, and 57.

why the correlation *r* became higher when wavelet preprocessing was applied.

*Evaluation in Long-term Use*

Figure 6 shows that the correlation between the measured and the estimated waveforms was high enough during the experiment. However, *r.m.s.e.* and *bias* became gradually larger in the last stage of the experiment. This result suggested that the method could simulate waveforms of flow rate sufficiently, but it needed an improvement to compensate for the bias error that might appear in the case of long-term use. Modification of preprocessing with wavelet filtering improved *r.m.s.e.* and *bias* a little, but their values were not yet acceptable for clinical use in which another calibration could not be performed in an implanted device.

It was revealed that the waveform of the flow rate is useful in detecting the suction,[14] and our result shows that these methods are effective even in long-term use, and estimated flow rate can be substituted. Also, the reverse flow shown in **Figure 5(b)** can also be detected with our method even in long-term use. Increase in the estimation error after POD 20 to 30 shown in **Figure 7** suggested that the increase was due to several reasons.

The first possible reason was the change in the operating point of the pump. In this experiment, flow rate decreased slightly as days passed by, so rotational speed was also con-

Table 1. *r.m.s.e.*, *r*, and *bias* in Figure 5 and Figure 8

| POD | *r.m.s.e.* [l/min] | *r* | *bias* [l/min] |
|---|---|---|---|
| 11 | 0.59 | 0.981 | 0.01 |
| 17 | 0.42 | 0.994 | -0.20 |
| 37 | 1.91 | 0.986 | 1.87 |
| 57 | 1.65 | 0.992 | 1.58 |

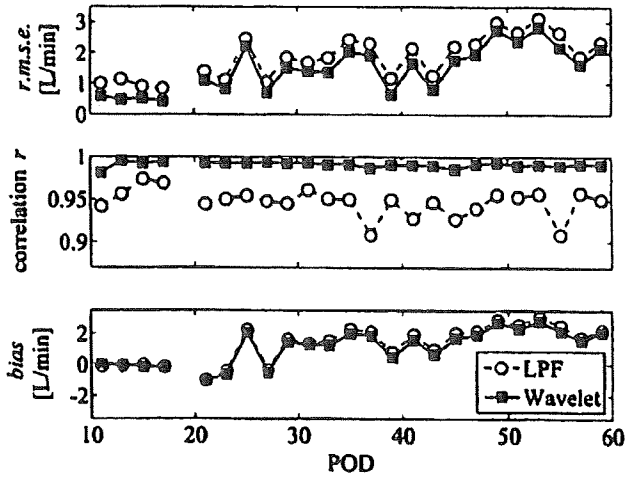


Figure 6. Trend of *r.m.s.e.*, *r*, and *bias* during the experiment (*solid line:* preprocessing with the wavelet filter; *dashed line:* low-pass filter. POD19: N/A).

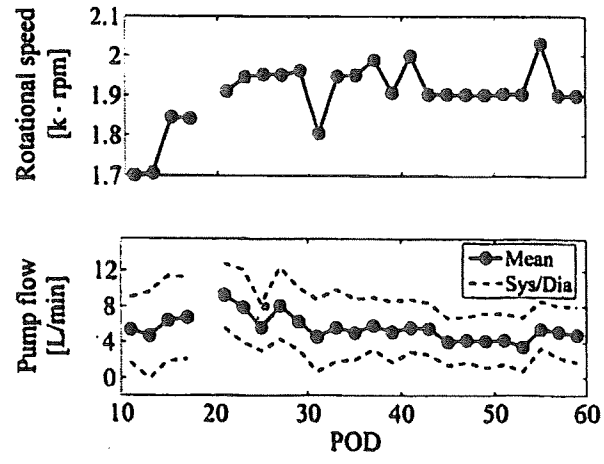


Figure 7. Trend of the operating point during the experiment (*top:* rotational speed; *bottom:* mean value of the flow rate; *dashed line* shows the peak value in systole/diastole).

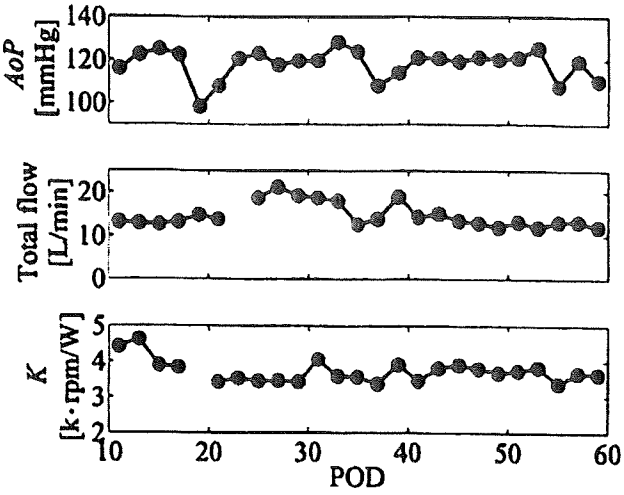


**Figure 8.** Trend of the average value of physiological data and gain *K* during the experiment (*top:* aortic pressure; *middle:* total flow measured at pulmonary artery; *bottom:* gain *K*).

trolled manually to keep a certain level of flow rate, as shown in **Figure 8.**

The second reason was mild intima formation at the outflow graft, which was found in the operation to wean the pumps on POD 63. Judging from the decrease in the amplitude of flow rate as shown in **Figure 7** and the change in its waveform, it could be speculated that the intima formation caused the partial obstruction of blood flow. The fact that a certain level of pump flow could be maintained throughout the experiment means this dimensional change due to intima formation was not critical for the VAD system.

In addition, the implantation of the VAD is so invasive that drastic change in physiological condition, such as vascular resistance and compliance, and regulation of the flow rate or pressure by the nervous system is possible. This is also not negligible. These problems can be avoided if we have enough data that include the wide range of operating points and various output resistances.

### *Limitation*

This experiment was performed with a healthy calf, but usually the VAD is implanted, not in a healthy person but in a patient in abnormal condition. An experiment with an animal with low cardiac function is preferred. However, such a condition is very difficult to prepare. Analysis in the interaction between the natural heart and the VAD[12,15] will be helpful to clarify the effect of the cardiac function against the accuracy of the estimation and improve the estimation method.

In this experiment, the data to identify the parameters of the estimator was obtained on PODs 11 and 13. In clinical use, however, it is impossible to measure flow rate after the implantation. The data used for identification should be obtained during surgery. It is desirable that generalized parameters for the estimation are approximated before the implantation. In addition, if a mock circulatory system could be built that simulates the physiological condition shown in these results, the system would also help to identify parameters more quickly and easily. However, even if such a precise mock system could be realized, the system would no longer be useful once the physiological condition varies. This is because online identification of the parameters included in the model without measuring the actual flow rate after implantation could not be performed.

Clarifying the conditions that must be included in the data for the identification of the parameters is important. Meanwhile, the data acquisition during the surgery should be as short as possible to prevent negative effect on the patient's condition. To interpolate the lack of data, some technique such as fuzzy logic or artificial neural networks will be helpful.

## Conclusion

The flow estimation method was evaluated with the data acquired from a chronic animal experiment. Estimation with good accuracy was confirmed until 15 days after the identification of the parameters. However, *r.m.s.e.* and *bias* started to increase during PODs 20 to 30, because of the change in the operating point and the partial obstruction of the cannula. This problem has to be solved by a more sophisticated method if this flow estimation method were to be used.

However, correlation $r$ was higher than 0.9 in all the acquired data, and estimated flow rate could simulate the profile of a measured one throughout the experiment. This information will be useful to detect an abnormal state during physiological monitoring, which does not always need an absolute value.

## Acknowledgments

This project was financially supported by the New Energy and Industrial Technology Development Organization (NEDO) under the Ministry of Economy, Trade, and Industry of Japan. D. Ogawa was supported by a grant of Tohoku University 21st COE Program: "Future Medical Engineering base on Bio-nanotechnology."

## References

1. Tsukiya T, Akamatsu T, Nishimura K, *et al*: Use of motor current in flow rate measurement for the magnetically suspended centrifugal blood pump. *Artif Organs* 21: 396–401, 1997.
2. Wakisaka Y, Okuzono Y, Taenaka Y, *et al*: Development of a flow estimation and control system of an implantable centrifugal blood pump for circulatory assist. *Artif Organs* 22: 488–492, 1998.
3. Ayre PJ, Vidakovic SS, Tansley GD, *et al*: Sensorless flow and head estimation in the VentrAssist rotary blood pump. *Artif Organs* 24: 585–588, 2000.
4. Kitamura T, Matsushima Y, Tokuyama T, *et al*: Physical model-based indirect measurements of blood pressure and flow using a centrifugal pump. *Artif Organs* 24: 589–593, 2000.
5. Funakubo A, Ahmed S, Sakuma I, Fukui Y: Flow rate and pressure head estimation in a centrifugal blood pump. *Artif Organs* 26: 985–990, 2002.
6. Tanaka A, Yoshizawa M, Abe K, *et al*: In vivo test of pressure head and flow rate estimation in a continuous-flow artificial heart. *Artif Organs* 27: 99–103, 2003.
7. Yoshizawa M, Sato T, Tanaka A, *et al*: Sensorless estimation of pressure head and flow of a continuous flow artificial heart based on input power and rotational speed. *ASAIO J* 48: 443–448, 2002.
8. Ayre PJ, Lovell NH, Woodard JC: Non-invasive flow estimation in

an implantable rotary blood pump: a study considering non-pulsatile and pulsatile flows. *Physiol Meas* 24: 179–189, 2003.
9. Tsukiya T, Taenaka Y, Nishinaka T, *et al*: Application of indirect flow rate measurement using motor driving signals to a centrifugal blood pump with an integrated motor. *Artif Organs* 25: 692–696, 2001.
10. Nose Y, Furukawa K: Current status of the gyro centrifugal blood pump: development of the permanently implantable centrifugal blood pump as a biventricular assist device (NEDO Project). *Artif Organs* 28: 953–958, 2004.
11. *Wavelet Toolbox* for use with MATLAB©, The Mathworks Inc; 2000.
12. Takahashi K, Uemura M, Watanabe N, *et al*: Estimation of left ventricular recovery level based on the motor current waveform analysis on circulatory support with centrifugal blood pump. *Artif Organs* 25: 713–718, 2001.
13. Asai T, Watanabe K, Ito S, *et al*: Real-time studies of the pivot bearings in the NEDO gyro PI-710 centrifugal blood pump. *Artif Organs* 28: 899–903, 2004.
14. Vollkron M, Schima H, Huber L, *et al*: Development of a suction detection system for axial blood pumps. *Artif Organs* 28: 709–716, 2004.
15. Nakata K, Shiono M, Akiyama K, *et al*: The estimation of cardiac function from the rotary blood pump. *Artif Organs* 25: 709–712, 2001.

日本バーチャルリアリティ学会第 11 回大会論文集 (2006 年 9 月)

# バーチャル・サイクリングチェア・システムに対する運動負荷に連動した仮想環境変化のための生体情報フィードバックの導入

Introduction of Bio-Feedback into a Virtual Cycling-Chair System for Adaptation to Chaining in Physical Load

佐藤 昇[1], 吉澤 誠[2], 田中 明[3], 高橋隆行[3], 関 和則[4], 半田康延[4]

Noboru SATO, Makoto YOSHIZAWA, Akira TANAKA, Takayuki TAKAHASHI, Kazunori SEKI and Yasunobu HANDA

1) 東北大学 大学院工学研究科 (〒 980-8579 仙台市青葉区荒巻字青葉 6-6-05, sato_n@yoshizawa.ecei.tohoku.ac.jp)

2) 東北大学 情報シナジセンター (〒 980-8579 仙台市青葉区荒巻字青葉 6-6-05, yoshizawa@ieee.org)

3) 福島大学 共生システム理工学類

4) 東北大学 大学院医学系研究科

**Abstract** : In the previous studies, the authors developed a rehabilitation system for patients impaired walking due to hemiplegia. In this system, the patients train themselves to move autonomously in a virtual environment. Pedaling speed and torque were used to evaluate the patient's riding skill and the motor function of his lower limbs. In the present study, a heart rate control has been introduced. Not only workload but also VR environment was changed simultaneously to avoid unnatural load regulation. We also have investigated change in blood pressure during the heart rate control to guarantee a safer rehabilitation system.

***Key Words:*** *Cycling-Chair, Biofeedback, VR-rehabilitation.*

## 1. はじめに

近年，ゲーム感覚を取り入れ，遊びながら高齢者や長期入院患者の心身の活性化を図る「遊びリテーション」[1] が関心を集めている.「遊びリテーション」は単調にならず，モチベーションを保ちながら，継続して運動できるという利点がある一方で，リハビリテーションの効率や安全性といった点は考慮されていないことが多く，特に高齢者や疾患者を対象とする場合は注意が必要である.

個人の運動能力・体力に合わせて運動療法を行うためには，ウォーミングアップおよびクールダウンの指示や過度な運動を避けるための心拍数の制御を行うのが一般的である. 砂川ら [2] は，エルゴメータの負荷を操作することにより，オーバーシュートを抑えつつ，できるだけ早く目標心拍数を維持するための自動制御方式を提案している. しかし，ペダルにかかるトルク変動だけで心拍数制御を行う環境は，単調であり対象者を飽きさせリハビリへの意欲向上が期待できない. より楽しく，できる限りアミューズメント性を維持するためには，シナリオを変化させることで自然な形で運動負荷を制御することが望ましい.

そこで本研究では，VR のアミューズメント性・インタラクティブ性を活かし，負荷変動に連動して VR 環境が変化することで，負荷変動が自然に感じられる運動療法を行うことができるリハビリシステムの構築を目的とした. さらに，心拍数制御時の収縮期血圧を計測し，生体情報フィードバックを積極的に利用し，より安全なシステムの構築に向けた検討を行った.

## 2. バーチャル・サイクリングチェア・システム

### 2.1 システムの概要

本研究で使用する VR リハビリシステムのシステム概略を図 1 に示す.

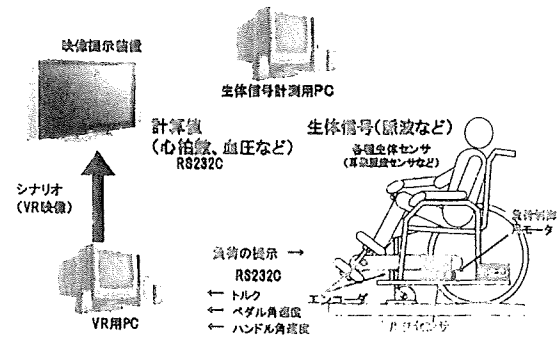


図 1: システム概要

システムはVR用PC，生体情報計測用PC，サイクリングチェアで構成される．計測量は，サイクリングチェア部に搭載されたマイコンにより，トルク，ペダル角およびハンドル角が，生体情報計測用PCで心拍数，血圧等の生体情報がVR用PCに送られ，負荷の決定とそれに応じたシナリオ変更を行う．運動負荷は，サイクリングチェア側に搭載されたマイコンにより，負荷提示用モータを制御して行う．

### 2.2 リハビリシナリオ

意欲向上を促すため，スポーツの持つアミューズメント性を着目した．心拍数制御を導入し，提示負荷に連動してVR環境が変化するシナリオ構築のためのプロトタイプとして川くだりシナリオを作成した．

ユーザーは傾斜角や流速が変化する川をペダルを漕いで下り，ゴールを目指す（図2）．運動負荷は心拍数がカルボーネンの式により定めた目標心拍数に近づくようにPI制御により決定される．この時提示負荷にあわせて提示される川の傾斜角や流速が変化する．

VR空間はOpen GLベースのWTK(Sense8製)を用いて作成した．

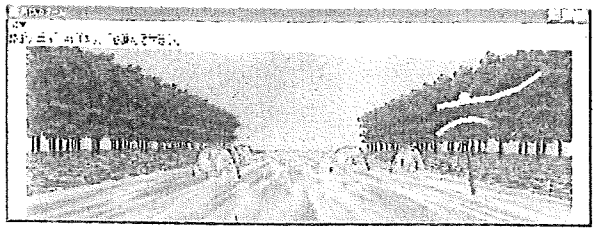

図2: VR川くだりシナリオ

## 3. 評価実験

被験者は健常者10名（男性9名，女性1名）で平均年齢23±2.0歳（22～28歳）である．

リハビリシナリオは3分間とし，ウォーミングアップおよびクールダウンとして前後に軽度の運動（仕事量15W，2分間）を行った．また，比較のため，十分に時間をおいてから，軽度の運動を行わなかった場合も測定した．

計測する生体情報は耳朶脈波による心拍数およびフィナプレス式連続血圧計（BV製，PORTAPRES）による連続血圧である．

目標心拍数はカルボーネンの式（$k = 0.3$）で設定した．

## 4. 結果および考察

３０秒毎の平均心拍数，平均収縮期血圧，平均脈波伝播時間差（耳朶脈波－指尖脈波）の安静時を基準とした変化を図3に示す．シナリオ実行中の心拍数は，いずれの被験者においても安定して目標心拍数を維持できており，本システムの負荷制御が良好であったことを示している．

また，前後に軽度の運動を行うことによって，それぞれの区間における心拍数の変動が穏やかになっていることがわかる．

一方，収縮期血圧は準備運動の有無で運動負荷中の値に約10mmHgの差が見られた．このことは，安全な運動療法において準備運動が重要であることを示しているばかりでなく，心拍数制御のみでは，このような血圧上昇を検出・抑制することが困難であること示している．すなわち，より安全なリハビリのためにはこのような血圧上昇を考慮する必要がある．

しかし，連続血圧を計測することは，現在のところ，高価かつ大掛かりな計測装置が必要であるため，リハビリ機器に導入することは困難である．簡単に計測できる脈波伝播時間は血圧と逆相関することが知られており，これを血圧の代用とすることも考えられる．しかし，本実験では，両者に弱い逆相関が見られたものの，収縮期血圧で見られた準備運動の有無による差は観察できなかった．

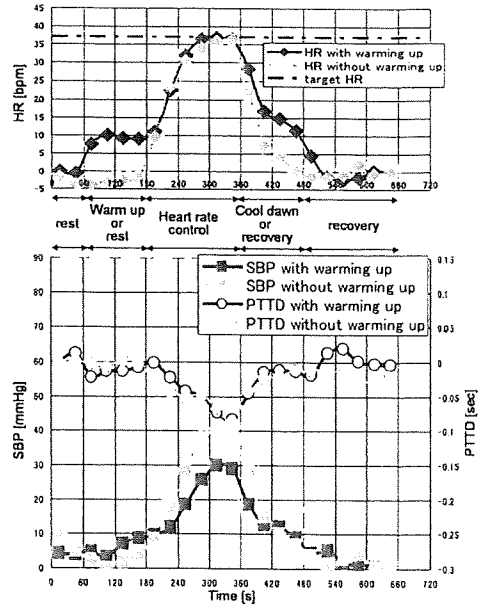


図3: シナリオ実行中の生体情報の変化

## 5. 終わりに

本研究では，心拍数フィードバックにより決定した負荷に連動してVR環境が変化する川くだりシナリオを作成した．シナリオが連動する心拍数制御は実現できたものの，心拍数制御のみでは抑制困難な血圧上昇が観測された．今後は，血圧制御のためのプロトコルを具体的に構築するとともに，脈波伝播時間を用いた血圧制御を検討し，より安全で手軽に運動療法を行えるシステムの構築が必要であると考えられる．

## 参考文献

[1] 三好春樹：遊びリテーション学，雲母書房，1999

[2] T Kawada, Y Ikeda, H Takaki, M Sugimachi, O Kawaguchi, T Shishido, T Sato, W Matsuura, H Miyano, and K sunagawa : Development of a servo-controller of heart rate using a cycle ergometer, Heart Vessels, Vol.14, No.4, pp.177-184, 1999.